Arch. Metall. Mater. **65** (2020), 2, 941-949

DOI: 10.24425/amm.2020.132842

A. SKOWRONEK[1], A. KOZŁOWSKA[1*], A. GRAJCAR[1], M. MORAWIEC[1]

MICROSTRUCTURE-PROPERTIES RELATIONSHIP AND MECHANICAL STABILITY OF RETAINED AUSTENITE IN THERMOMECHANICALLY PROCESSED MEDIUM-C TRIP STEEL AT DIFFERENT DEFORMATION TEMPERATURES

The paper presents the effect of deformation temperature on the mechanical stability of retained austenite in a multiphase TRIP steel. Series of static tensile tests were carried out in the temperature range –20 to 140°C in order to simulate the temperatures occurring during stamping process of automotive steel sheets and conditions of their exploitation. Samples deformed at 20°C and 60°C showed the best combination of strength and ductility. It was related to the gradual transformation of retained austenite into martensite. Obtained results revealed that the intensity of TRIP effect is significantly related to the deformation temperature. The amount of retained austenite, which transformed into martensite during plastic deformation decreases as the deformation temperature increases. It was also found that the stability of retained austenite depends on its morphology. The obtained results showed the relationship between deformation temperature and the stability of retained austenite. The chemical composition and microstructure of multiphase steels dedicated to the automotive industry should be designed for providing the maximum TRIP effect at the specific deformation temperatures.

Keywords: TRIP effect, multiphase steel, retained austenite, mechanical stability, deformation temperature

1. Introduction

The growing requirements of the automotive industry regarding the increase of passenger's safety during the crash events and the reduction of fuel consumption lead to developing steels, which are characterized by high strength and good formability [1-7]. These advantages have multiphase TRIP (Transformation Induced Plasticity) steels which belong to the AHSS group (Advanced High Strength Steels). A variety of phases showing different strength properties such as ferrite (50-60%), bainite (25-40%) and retained austenite (5-15%) ensure high strength (in the range 700-1200MPa) and good formability (elongation up to 35%). Retained austenite is a key microstructural component which progressively transforms into martensite during plastic deformation. It provides the high work hardening rate of the steel [8-12].

The additional increase in strength properties can be obtained by increasing the bainite content in relation to the ferritic matrix [13-17]. For this purpose, the carbon content should be increased. A higher carbon content affects also the possibility of obtaining a higher amount of retained austenite. It is related to the fact that carbon is an austenite stabilizer [18-22]. The disadvantage of this solution is that with increasing C content there is a significant deterioration in the weldability of steel [22,23]. It reduces possible technologies which can be applied for the production of final components.

An important issue from the effectiveness point of view of the TRIP effect is a stability of this phase. It depends on several factors which can be classified as internal (chemical composition, grain size, matrix type, morphology) and external (stress state, strain rate and deformation temperature) [9,23-26]. The strain level at which austenite transforms into martensite is related to the carbon content in this metastable phase. The retained austenite (RA) characterized by a low carbon content easy transforms into martensite, even at low strain levels. It results in reduced steel ductility. On the other hand, RA characterized by a high carbon content is much more stable, thus it does not transform into marteniste even at high strain levels. In this case, the RA stays stable during deformation, thus the TRIP effect does not occur during forming operations or crash events [5,27,28].

Other important factor is a deformation temperature which has so far been less emphasized in the available literature. Thus,

[1] SILESIAN UNIVERSITY OF TECHNOLOGY, DEPARTMENT OF ENGINEERING MATERIALS AND BIOMATERIALS, 18A KONARSKIEGO STR., 44-100 GLIWICE, POLAND

* Corresponding author: aleksandra.kozlowska@polsl.pl

the present paper aims at determining changes in the mechanical stability of RA at different deformation temperatures, which reflect technological windows of manufacturing conditions (sheet stamping, bending, etc.) or service conditions at decreased or increased temperatures.

2. Material and experimental procedures

The investigated material was 0.43C-1.45Mn-1Si-1Al-0.033Nb-0.01Ti steel. The increased carbon content was applied to obtain a greater ratio of carbide-free bainite to ferritic matrix as well as an increased amount of RA [13,14,29]. Nb and Ti microadditions were added to obtain grain refinement (by precipitation and inhibition of recrystallization during hot-working).

The ingots were melted using vacuum induction furnace and then they were hot forged to a thickness of 22 mm. In the next step, the flat samples were roughly rolled to a thickness of 4.5 mm in the temperature range 1200-900°C. The thermomechanical rolling was conducted in 3 passes and the final sheet thickness was 2 mm. A detailed information concerning the processing parameters can be found in works [13,14] and in the scheme shown in Fig 1. Results of calculations performed by using the JMatPro software showed that the M_s temperature of steel was about 316°C. A carbon content in retained austenite was 1.52%C giving its $M_{s\gamma}$ temperature: –118°C [14]. It provided its thermal stability during tensile tests at all applied deformation temperatures.

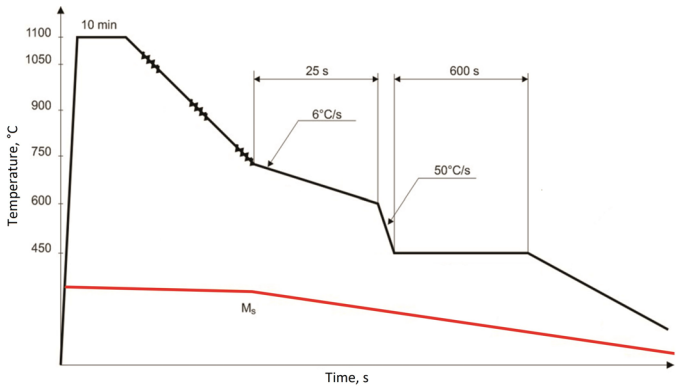

Fig. 1. Scheme of thermomechanical processing of the investigated steel

In order to examine the effect of deformation temperature on the mechanical properties of investigated steel, series of static tensile tests carried out at a strain rate of 5×10^{-3} s^{-1} were performed. Experiments were performed at room (20°C), reduced (–20 °C) and elevated (60°C, 100°C and 140°C) temperatures using the Zwick Z/100 testing machine equipped with an environmental chamber. Flat samples of 2 mm thick, 50 mm gauge length and 12.5 mm width were used for the tests. The test temperature range was chosen to reflect the processing conditions of steel sheets where the temperature of the element increases as a result of friction.

Observations of the microstructure of investigated steel at the initial state and after static tensile tests were carried out to determine the effect of plastic deformation temperature on the tendency of RA to martensitic transformation. The deformed microstructures were observed along the tensile direction. A Leica MEFa light microscope was used for metallographic observations. Detailed morphology of bainite was revealed using scanning electron microscopy (ZEISS Supra 25 SEM). The samples for microstructural analysis were cut from the necking area. They were prepared by using standard metallographic procedures. Nital and sodium pyrosulfate reagents were used to reveal the ferrite grain boundaries and other individual phases. The final stage of microstructural observations was the image analysis of etched samples using Image-Pro Plus 6.0. It enables assessing the amount of individual phases and the stereological parameters of the retained austenite based on the differences in phase colors resulting from etching.

The analysis allowing determination of the amount of formed strain-induced martensite during plastic deformation was carried out in a 0-1 mode (0 – means not transformed, 1 – means transformed). The grains in which even a partial martensitic transformation took place were considered as the transformed grains (1). The amount of retained austenite in the deformed specimens was relatively compared to the reference microstructure at the initial state (100%) in order to assess an amount of the austenite transformed into martensite during deformation. The additional digital processing was applied to improve the quality of the analyzed microstructure.

3. Results and discussion

3.1. Mechanical properties at different deformation temperatures

Results of the static tensile tests performed in a temperature range -20-140°C are shown in Fig. 2. Obtained mechanical properties are summarized in Table 1. It was found that deformation temperature affects significantly the mechanical properties (Fig. 2a). The lowest strength and ductility were obtained for specimens deformed at the highest temperatures: 100 and 140°C. The best mechanical properties showed specimens deformed at 20 and 60°C. The highest values of total elongation (18.3 and 19.1%, respectively) were obtained at these deformation temperatures. One can see in Fig. 3 that the deformation temperature affects most significantly total elongation values and

TABLE 1

Mechanical properties of investigated steel at different deformation temperatures

Deformation temperature, °C	YS, MPa	UTS, MPa	TEl, %
-20	536	853	15.8
20	540	889	18.3
60	502	818	19.1
100	490	719	17.1
140	475	702	17.3

tensile strength, whereas to a smaller extent the yield strength values. Zhu et al. [30] also observed in 0.2C-2Mn-1.6Si type steel that the mechanical properties decrease as the deformation temperature increases.

The deformation temperature strongly affects the work hardening rate of investigated steel (Fig. 2b). The $d\sigma$-$d\varepsilon$ values decrease gradually as the deformation degree increases. The work hardening rate is strongly related to the intensity of TRIP effect which depends on the stability of retained austenite. The smallest slop of the tensile curve was obtained at 20°C. It is related to the gradual transformation of retained austenite into martensite during deformation. The gradual transformation of γ phase into martensite was observed in our previous work [13]. A slightly higher slope of curves was observed for the specimens deformed at –20 and 60°C. With increasing the deformation temperature to 100°C and 140°C, the general slope of $d\sigma$-$d\varepsilon$ curves rises. It is related to the increasing austenite stability with an increase in deformation temperature.

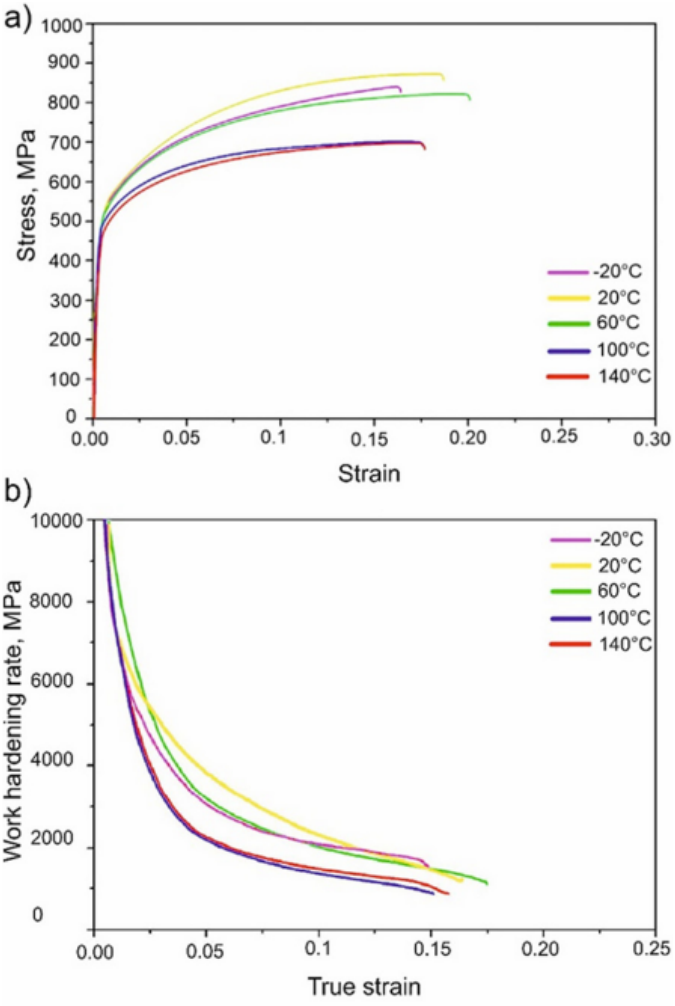

Fig. 2. Engineering stress-strain curves (a) and work hardening rate as a function of true strain (b) at various deformation temperatures

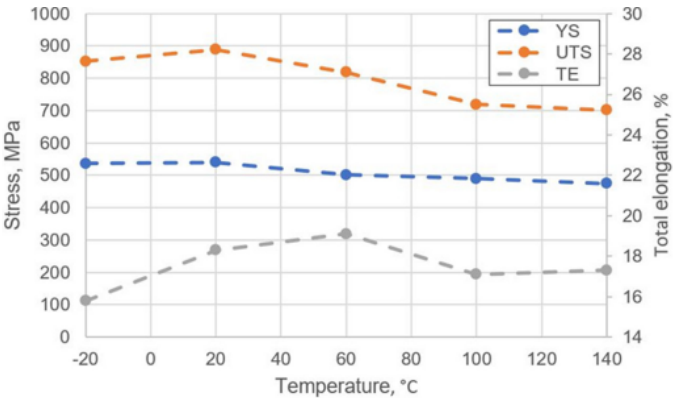

Fig. 3. Changes in mechanical properties as a function of deformation temperature

3.2. The microstructure of investigated steel after thermomechanical treatment

The initial microstructure of investigated steel is presented in Fig. 4. The specimens were prepared along the rolling direction (Fig. 4a). For all microscopic images presented in the paper, both rolling and static tensile testing (deformed samples) were horizontally. The steel is characterized by fine-grained ferritic-bainitic microstructure with a large amount of retained austenite (Fig. 4b). The matrix is ferrite characterized by different sizes of granular grains, slightly elongated according to the rolling direc-

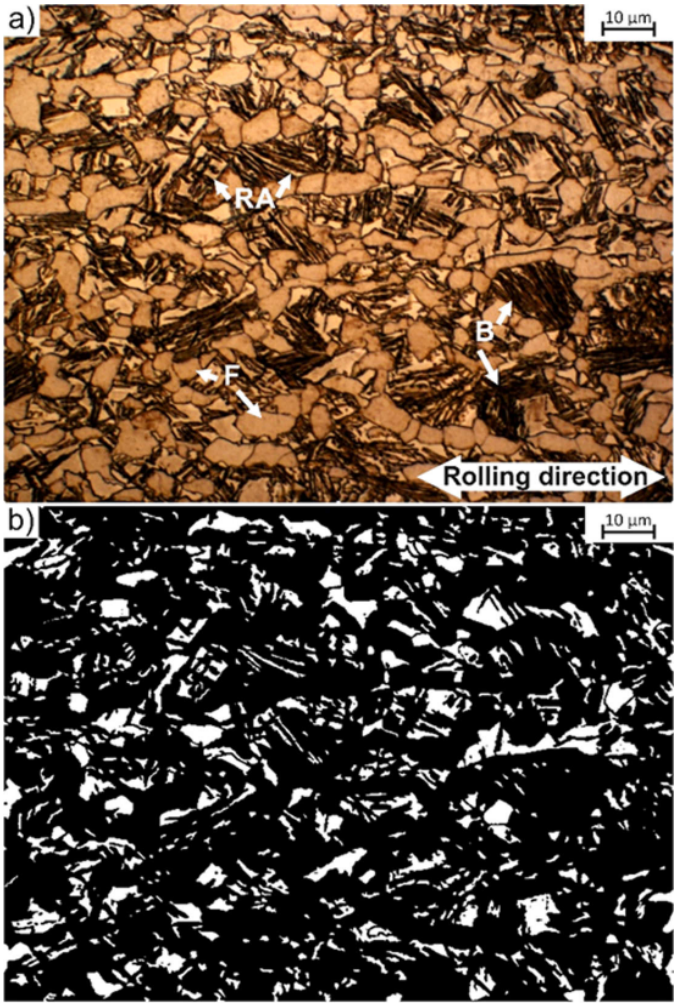

Fig. 4. Initial microstructure of the investigated steel: a) optical micrograph; b) binary map of retained austenite (marked as white)

tion. The majority of ferrite grains is lower than 8 μm due to some grain refinement by the inhibition of austenite recrystallization during hot rolling caused by Nb-Ti carbonitrides [14] and the successive $\gamma \rightarrow \alpha$ transformation. However, the grain refinement effect is not pronounced because the total addition of Nb and Ti is lower than 0.05%. RA in a form of blocky grains is located at bainitic areas or between ferrite grains. Retained austenite as thin layers is located between bainitic laths (Fig. 4b). The presence of carbide-free bainite and interlath retained austenite was confirmed by the SEM micrograph in Fig. 5. The carbides (typical for the conventional bainite) are replaced by continuous or interrupted layers of retained austenite.

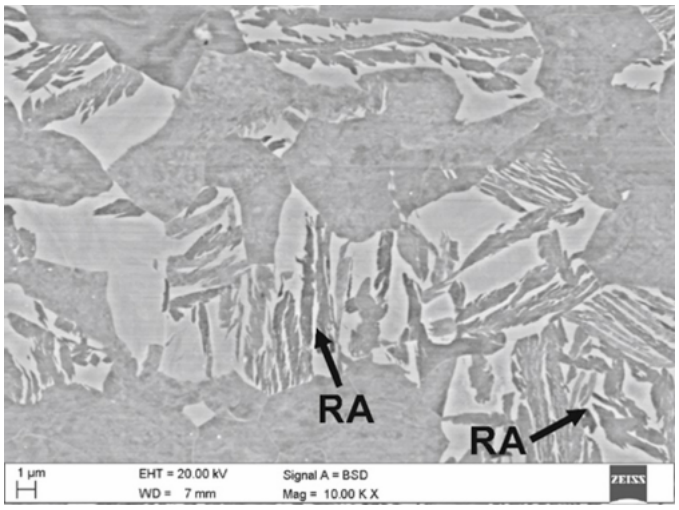

Fig. 5. The SEM micrograph showing the morphology of bainitic islands

The amount of RA at the initial microstructure was estimated to be ca. 19.2%. There is some overestimation of this parameter (~2%). The slightly smaller amount result was measured in our earlier work [14] by using the XRD method (17.6%). Histograms characterizing the RA features are presented in Fig. 6. It was noted that despite the large amount of grains smaller than 3 μm^2, these grains do not have a significant impact on the surface share of γ phase. The surface share of RA grains smaller than 1 μm^2, 1-2 μm^2 and 2-3 μm^2 is about 1%. A large fraction of RA grains lower than 5 μm^2 is a result of the γ phase as thin layers located in bainitic areas. The largest contribution to the surface share (approx. 12%) have grains larger than 10 μm^2, despite the fact that they occur in an amount of 0.4 grains / 100 μm^2 (Fig. 6a).

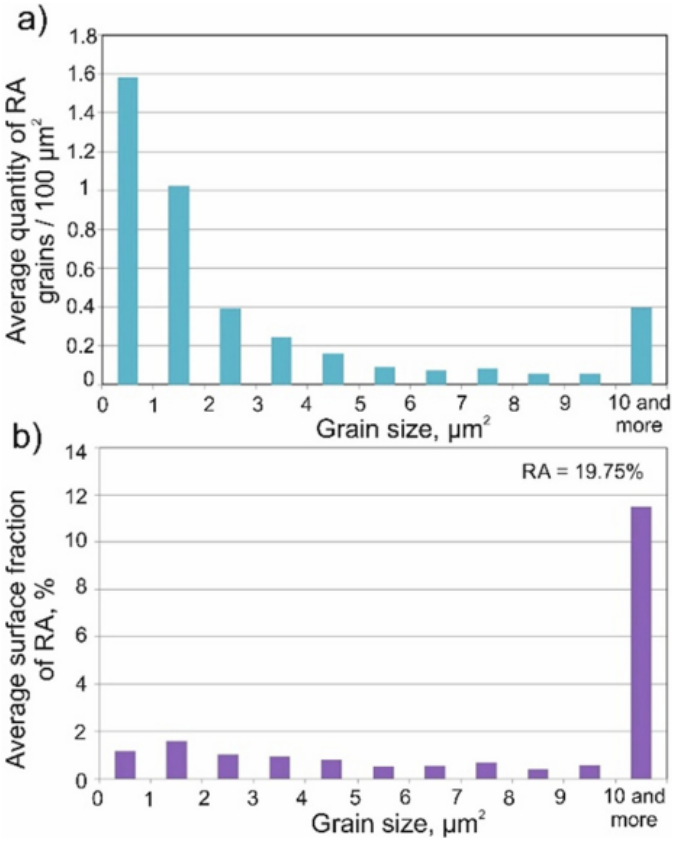

Fig. 6. Statistical evaluation of RA parameters at the initial state: a) average quantity of RA grains per 100 μm^2, b) average surface fraction of RA

3.3. Microstructures of specimens deformed at different temperatures

The image analysis of deformed samples allowed to estimate the surface share of individual microstructural components of investigated steel, which are summarized in Table 2. The applied method for evaluating the amount of retained austenite is affected by some measurement errors. However, the amount of retained austenite determined in our earlier work using the XRD method at the initial state is similar, i.e., 17.6% [14]. The difference is about 2%. The obtained results showed the tendency to stabilize the retained austenite with increasing deformation temperature, which is also consistent with the results obtained by other authors [31].

TABLE 2

Amount of RA at various deformation temperatures

Amount of retained austenite at initial microstructure = 19.2 %						
Deformation temperature, C°	**V_{RA}, %**	**V_M, %**	**$V_{RA} + V_M$, %**	*** Amount of RA transformed into martensite**		**The smallest RA grain size transformed into martensite during deformation, μm^2**
				In relation to the initial state	**In relation to microstructures after deformation**	
–20	8.8	9.2	18.0	0.57	0.51	<1
20	11.2	7.0	18.2	0.42	0.38	<1
60	13.5	5.2	18.7	0.30	0.29	<1
100	17.0	2.6	19.6	0.11	0.14	1-2
140	18.7	1.9	20.6	0.03	0.10	3-4

V_{RA} – amount of retained austenite; V_M – amount of martensite

In order to increase the reliability of the obtained results, the relative fraction of austenite which transformed into martensite during plastic deformation was compared to the microstructure of the specimen at the initial state. It means that the initially determined 19.2% volume fraction of retained austenite constitutes 100% total retained austenite. It is a little bit different compared to the combined fractions of retained austenite and formed martensite ($V_{RA} + V_M$) determined for the plastically deformed samples. It is better to use the initial retained austenite fraction as the reference due to more complicated determination of the total amount of untransformed austenite and the resulting martensite on the plastically deformed samples. That is why the ($V_{RA} + V_M$) sometimes did not correspond exactly to the initial share of retained austenite at the initial microstructure.

In the case of a sample deformed at –20°C (Fig. 7) a large amount of retained austenite in a form of thin layers located between bainitic laths can be distinguished in the microstructure. This is clear when analyzing the figures 7a and 7b together. Blocky-type grains of retained austenite are located near bainitic islands or ferrite grains. In comparison to the initial microstructure, the analyzed image shows the presence of martensite which

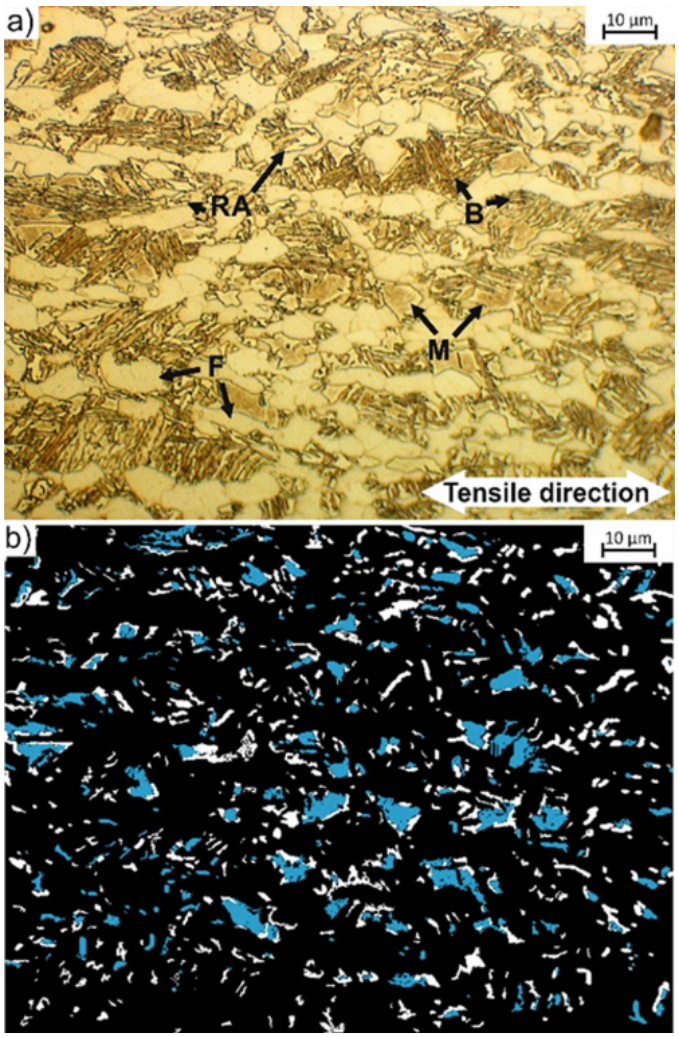

Fig. 7. Microstructure of the investigated steel deformed at –20°C: a) optical micrograph, b) binary map of retained austenite (white) and martensite (blue)

is formed as a result of the TRIP effect. The quantity of retained austenite and martensite was evaluated based on the binary map (Fig. 7b). This transformation occurred mainly in large blocky austenite grains, while thin layers of γ phase located in bainitic islands remained stable (Fig. 7b). A lack of transformation of lath austenite into martensite results from their small size and location between hard bainite laths. The stability of retained austenite is related to the size of austenitic grains. Due to the fragmentation of larger grains of γ phase by the newly formed martensite, new fine-grained areas of RA characterized by even higher stability were formed. It was found in works [31,32], that the blocky-type retained austenite had lower carbon contents than a film-type RA, thus it easier transforms into martensite. Moreover, Das et al. [33] reported that blocky RA possesses some fraction of microstructural defects, like dislocations and stacking faults which constitute the martensite nucleation zones. It was also found in the present study that mainly the central areas of the blocky-type retained austenite were transformed, whereas areas at the grain boundaries remained stable. Similar results were observed in work [34]. It is related to the increased carbon content of areas near grain boundaries as a result of a smaller carbon diffusion path from the α phase regions. Central parts of retained austenite easier transform into martensite due to their lower stability. Ferrite grains are visible elongated according to the tensile direction, whereas bainite and martensite show no significant deformation effects.

At deformation temperature –20°C, the retained austenite is characterized by relatively low mechanical stability. The transformation of retained austenite into martensite occurs intensively in large blocky grains. The freshly formed martensite with the relative surface share ca. 55% led to a strong fragmentation of austenitic areas, resulting in a dominant share of RA grains smaller than 6 μm^2 (Fig. 8b). In comparison to the initial microstructure, it should be noted that the amount of grains larger than 10 μm^2 decreased significantly (Fig. 7a). The minimum grain size of γ phase transformed into martensite during deformation was smaller than 1 μm^2 (Tab. 2). The intensity of strain-induced martensitic transformation is demonstrated in Fig. 8c. It can be seen that almost all large grains (8 μm^2 and larger) are transformed (it means that the transformation is initiated) but the transformation in the individual grain volumes took place only partially. The surface share of RA was estimated to be ca. 8.8% (Fig. 8b).

Fig. 9a shows the microstructure of the sample deformed at room temperature. Similarly to the microstructure deformed at reduced temperature (–20°C), martensite was formed in large blocky grains of RA surrounded by ferrite and at bainitic islands. The presence of soft ferrite affects the easier transformation into martensite [35]. One can see that the central areas of blocky grains of RA were transformed, whereas the areas near grain boundaries stayed stable (Fig. 9b).

The surface share of retained austenite after deformation was estimated to be ca. 11.2% (Fig. 10). The relative surface share of the freshly formed martensite was about 43% when compared to the initial microstructure. It means that the me-

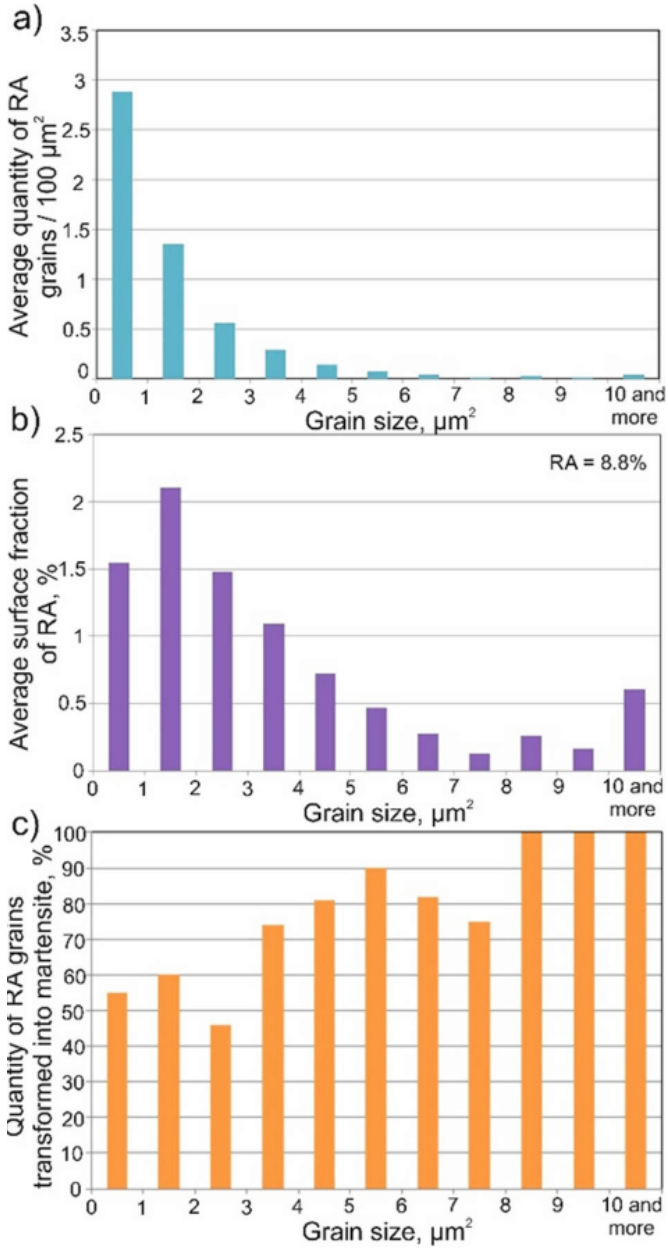

Fig. 8. Statistical evaluation of RA parameters at –20°C: a) average quantity of RA grains per 100 µm^2; b) average surface fraction of RA; c) quantity of retained austenite grains transformed into martensite

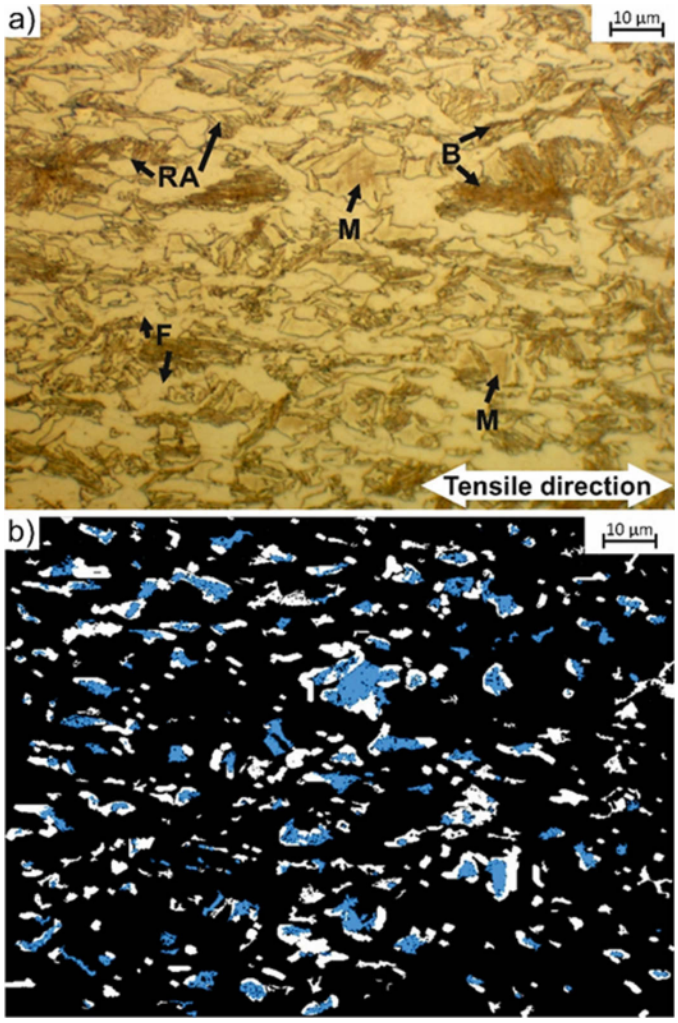

Fig. 9. Microstructure of the investigated steel deformed at 20°C: a) optical micrograph, b) binary map of retained austenite (white) and martensite (blue)

chanical stability of the γ phase increased slightly with increasing deformation temperature (Tab. 2).

The tendency to martensitic transformation of RA grains smaller than 7 µm^2 is lower in comparison to the specimen deformed at –20°C (Fig. 10c). It is caused by a lower tendency to martensitic transformation of grains located at bainitic islands. Large blocky grains almost all transformed into martensite, while the smallest austenite grains (smaller 3 µm^2) remain in approx. 18% unchanged. The minimum grain size of γ phase transformed into martensite during deformation was smaller than 1 µm^2 (Tab. 2).

In case of the steel deformed at elevated temperatures: 100°C (Fig. 11) and 140°C (Fig. 13), the amount of untransformed retained austenite is ca. 17.0 and 18.7%, respectively. The γ phase stability rises with increasing temperature and less amount of RA transformed into martensite when compared to the lower deformation temperatures. Only the largest grains of retained austenite transformed into martensite during deformation (Fig. 11b and 13b). Austenite islands smaller than 1 µm^2 at 100°C and 3 µm^2 at 140°C remained stable, whereas the largest blocky austenite grains transformed in 90% and 70%, respectively (Fig. 12c and 14c). The minimum grain size of γ phase transformed into martensite during deformation at 140°C was smaller than 3-4 µm^2 (Tab. 2).

The intensity of the TRIP effect decreased with an increase in deformation temperature. It is related to the increase of the stacking fault energy (SFE) value resulting in a higher stability of retained austenite [36]. The same tendency was also observed in other AHSSs grades [37,38]. The largest grains of RA transformed only partially into martensite. The small grains and thin layers of this phase remained stable (Tab. 2). The average carbon content in retained austenite was 1.52% C [14] while the corresponding martensite start temperature: –118°C. It means that the calculated $M_{s\gamma}$ temperature of γ phase provided its thermal stability in the range of deformation temperatures applied in the

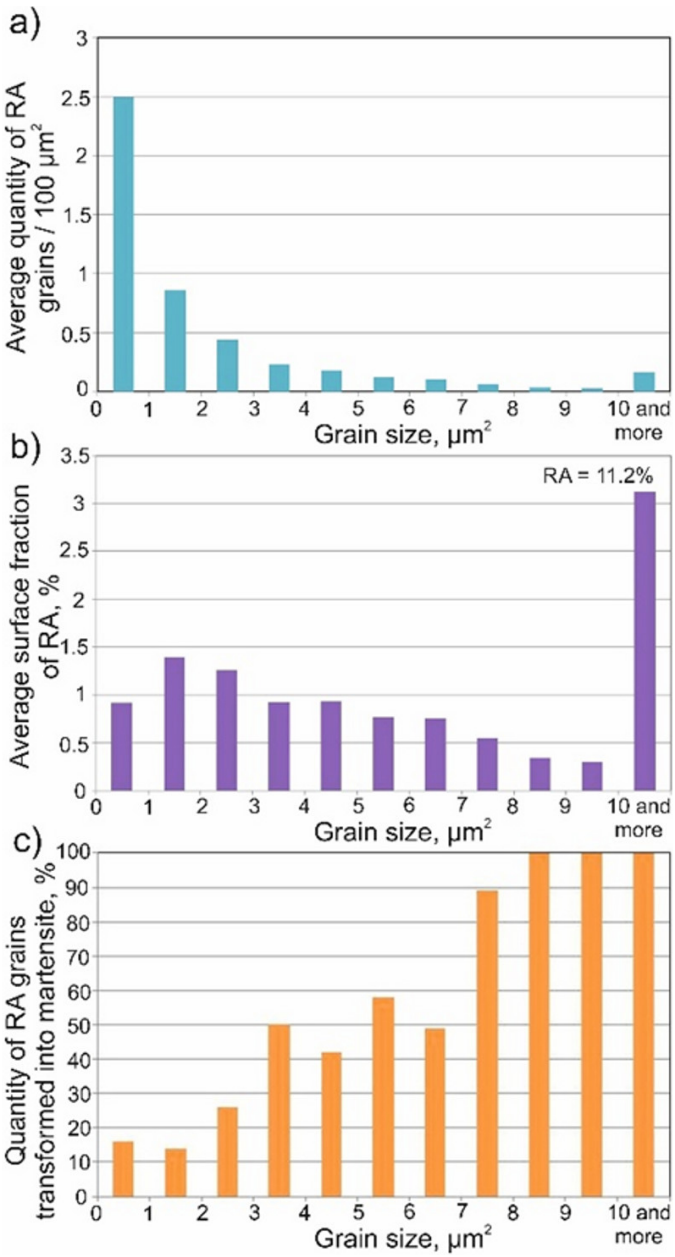

Fig. 10. Statistical evaluation of RA parameters at 20°C: a) average quantity of RA grains per 100 μm^2; b) average surface fraction of RA; c) quantity of retained austenite grains transformed into martensite

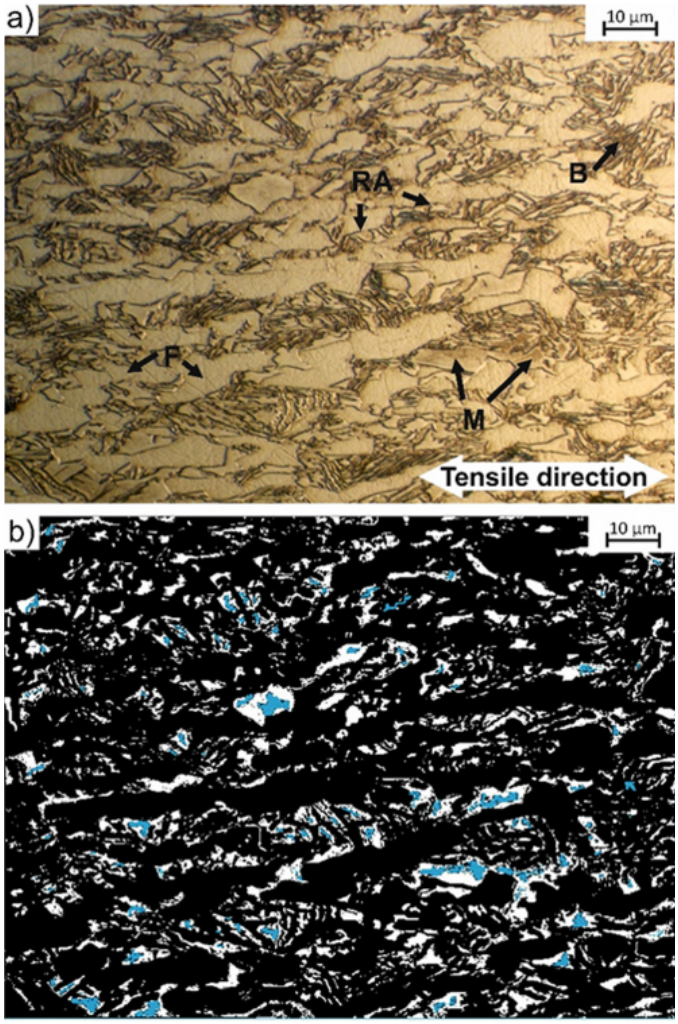

Fig. 11. Microstructure of the investigated steel deformed at 100°C: a) optical micrograph, b) binary map of retained austenite (white) and martensite (blue)

static tensile tests. Therefore, martensitic transformation took place as a result of plastic deformation being strongly dependent on the retained austenite grain size and morphology.

4. Conclusions

A series of tensile test was performed for the thermomechanically processed medium-C TRIP steel in a temperature range from –20°C to 140°C. The tendency of the retained austenite with a $M_{s\gamma}$ temperature below –100°C to the strain-induced martensitic transformation was determined. The obtained results showed that the stability of retained austenite strongly depends on the deformation temperature. An increase in the deformation temperature resulted in a reduced intensity of the TRIP effect due to higher mechanical stability of RA. The highest fraction of RA transformed into martensite at –20°C, whereas the lowest intensity of martensitic transformation was observed at the highest deformation temperature: 140°C. It was found that the tendency to martensitic transformation is strongly related to the austenite morphology and grain size. RA in the form of thin layers located between bainitic laths was characterized by higher stability than blocky retained austenite. Martensitic transformation occurs most intensively in the central area of large blocky-type austenitic grains located in the ferritic matrix. When the deformation temperature increases a size of untransformed RA grains increases. At low deformation temperatures, only the smallest RA grains remained stable after deformation.

The most beneficial combination of strength and ductility was observed in specimens deformed at 20 and 60°C. It is related to the gradual transformation of retained austenite into martensite during deformation which ensures the favorable work hardening rate. The lowest mechanical properties were obtained in the specimens deformed at the highest temperatures 100 and 140°C due to the lower intensity of the TRIP effect.

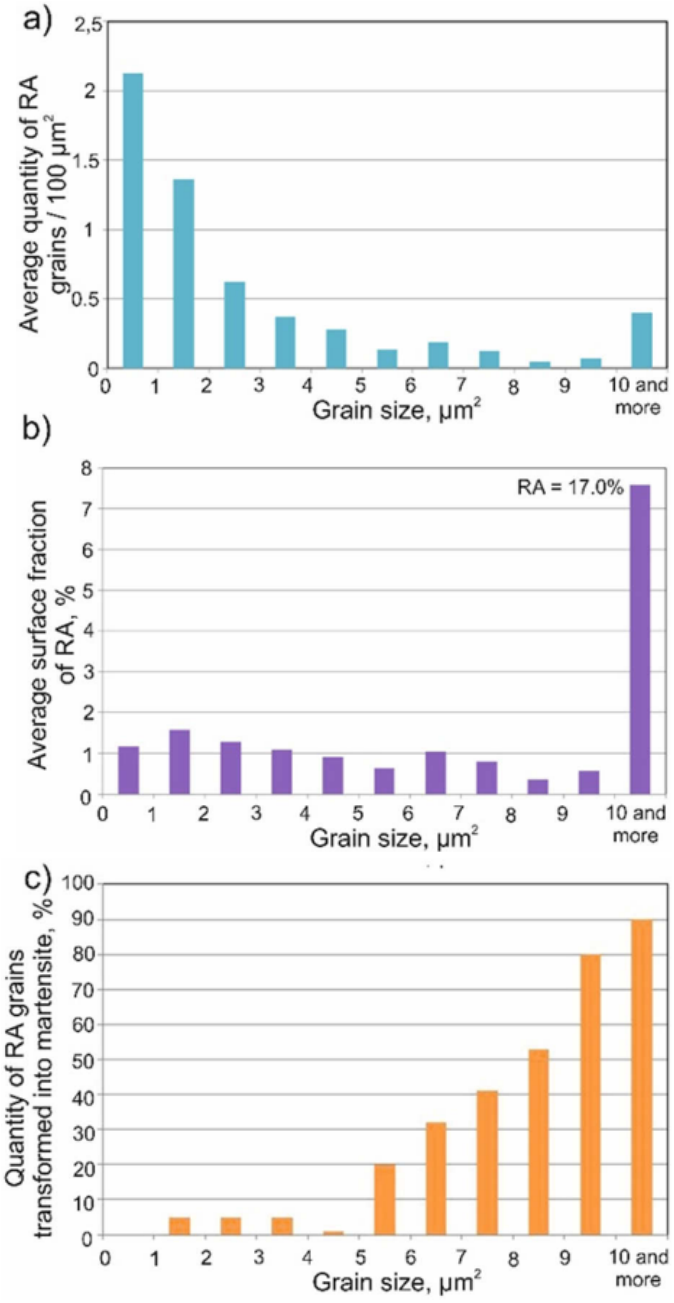

Fig. 12. Statistical evaluation of RA parameters at 100°C: a) average quantity of RA grains per 100 µm^2; b) average surface fraction of RA; c) quantity of retained austenite grains transformed into martensite

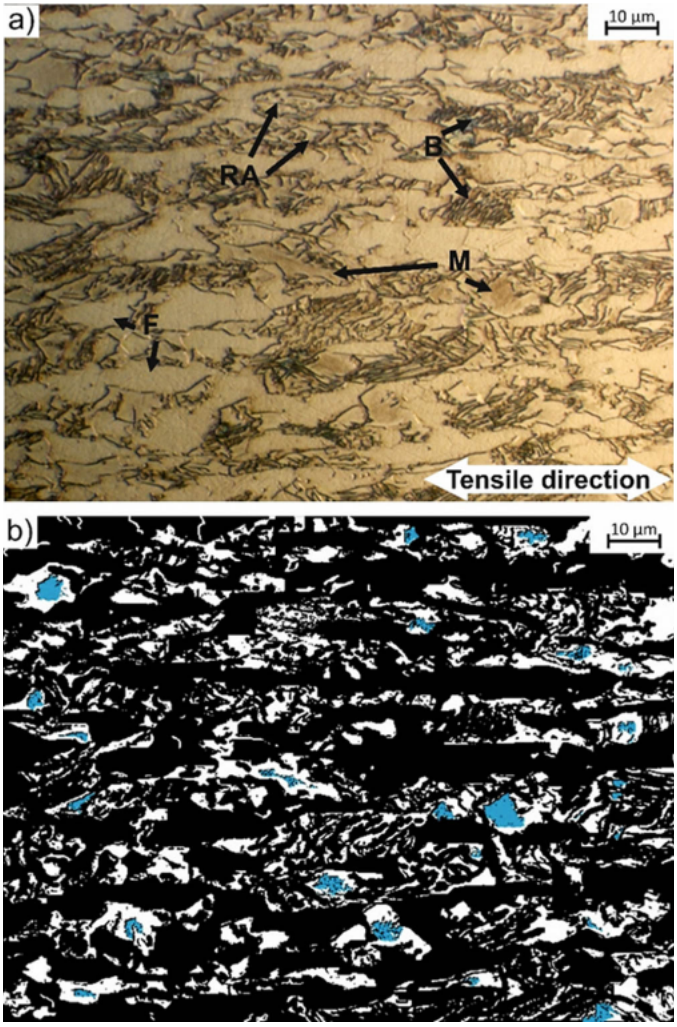

Fig. 13. Microstructure of the investigated steel deformed at 140°C: a) optical micrograph, b) binary map of retained austenite (white) and martensite (blue)

Acknowledgments

A. Kozłowska acknowledges the support from statutory funds of the Faculty of Mechanical Engineering of Silesian University of Technology in 2019.

REFERENCES

[1] A. Grajcar, S. Lesz, Mater. Sci. Forum **706-709**, 2124-2129 (2012).
[2] B.C. De Cooman, Curr. Opin. Solid. St. **8**, 285-303 (2004).
[3] R. Kuziak, R. Kawalla, S. Waengler, Arch. Civ. Mech. Eng. **8**, 2, 103-117 (2008).
[4] Z. Gronostajski, A. Niechajowicz, S. Polak, Arch. Metall. Mater. **55**, 1, 221-230 (2010).
[5] S. Keeler, M. Kimchi, Peter J. Mooney, Advanced high-strength steels application guidelines version 6.0, WorldAutoSteel 2017.
[6] K. Kowalczyk, M. Jabłońska, S. Rusz, G. Junak, Arch. Metall. Mater. **63**, 4, 1957-1961 (2018).
[7] M. Hojny, M. Glowacki, P. Bała, W. Bednarczyk, W. Zalecki, Arch. Metall. Mater. **64**, 1, 401-412 (2019).
[8] E. Hadasik, R. Kuziak, R. Kawalla, M. Adamczyk, M. Pietrzyk, Steel Res. Int. **77**, 927-933 (2006).
[9] E.V. Pereloma, A.A. Gazder, I. Timokhina, Retained austenite: Transformation-Induced Plasticity, Encyclopedia of Iron, Steel, and Their Alloys. Taylor and Francis, New York 2016.
[10] A. Grajcar, M. Kciuk, S. Topolska, A. Płachcińska, J. Mater. Eng. Perform. **25**, 6, 2245-2254 (2016).
[11] M. Adamczyk, D. Kuc, E. Hadasik, Arch. Civ. Mech. Eng. **8**, 3, 5-13 (2008).
[12] J. Jung, S.J. Lee, S. Kim, B.C. De Cooman, Steel Res. Int. **82**, 857-865 (2011).
[13] A. Grajcar, Mater. Tehnol. **49**, 5, 715-720 (2015).

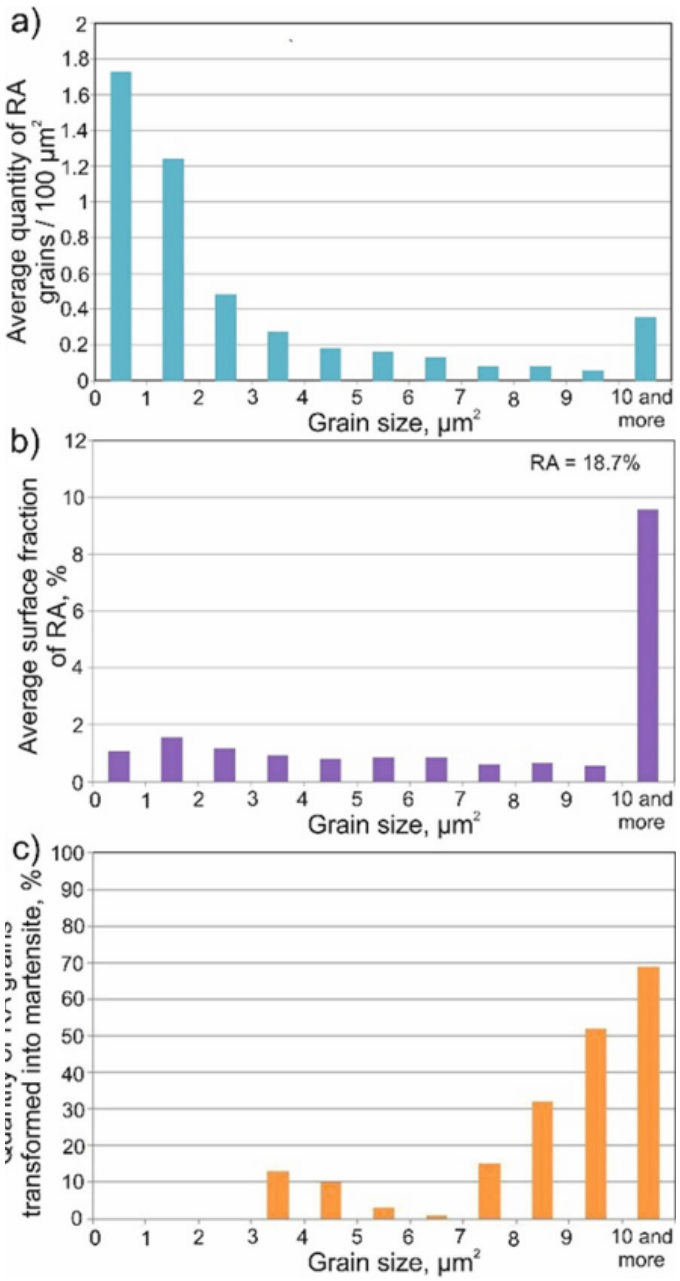

Fig. 14. Statistical evaluation of RA parameters at 140°C: a) average quantity of RA grains per 100 µm^2; b) average surface fraction of RA; c) quantity of retained austenite grains transformed into martensite

[14] A. Grajcar, W. Kwaśny, W. Zalecki, Mater. Sci. Tech. **31**, 7, 781-794 (2015).

[15] C. Garcia-Mateo, F.G. Caballero, ISIJ Int. **45**, 1736-1740 (2005)

[16] K. Radwański, R. Kuziak, R. Rozmus, Arch. Civ. Mech. Eng. **19**, 2, 453-468 (2019).

[17] H. Nasr El-Din, E.A. Showaib, N. Zaafarani, IJMME. **12**, 3-12 (2017).

[18] A. Grajcar, P. Skrzypczyk, D. Woźniak, Arch. Metall. Mater. **59**, 4, 1691-1697 (2014).

[19] A. Kokosza, J. Pacyna, Mater. Sci. Technol. **31**, 7, 802-807 (2015).

[20] L. Kucerova, H. Jirkova, A. Jandova, Acta Metall. Mater. **23**, 3, 244-252 (2017).

[21] A. Kurc-Lisiecka, A. Lisiecki, Mater. Perform. Charact. **8**, 6, 1-11 (2019).

[22] J. Gorka, S. Stano, Metals **8**, 2, 132-147, doi: 10.3390/met8020132 (2018).

[23] A. Grajcar, K. Radwański, Mater. Tehnol. **48**, 5, 679-683 (2014).

[24] S. Chen, Z. Cao, C. Wang, C. Huang, D. Ponge, W. Cao, J. Iron Steel Res. Inst. **26**, 1209-1218 (2019).

[25] A. Kokosza, J. Pacyna, Arch. Metall. Mater. **55**, 1001-1006 (2010).

[26] M.N. Yoozbashi, T. Hajilou, E. Akbarzadeh Chiniforush, S. Yazdani, ISSI Int. **14**, 2, 27-32 (2017).

[27] F.G. Caballero, C. Garcia-Mateo, J. Chao, M.J. Santofimia, C. Capdevila, C.G. de Andres, ISIJ Int. **48**, 1256-1262 (2008).

[28] C. Garcia-Mateo, F.G. Caballero, J. Chao, C. Capdevila, C. Garcia de Andres, J. Mater. Sci. **44**, 17, 4617-4624 (2009).

[29] S. Zaefferer, J. Ohlert, W. Bleck, Acta Mater. **52**, 9, 2765-2778 (2004).

[30] D.X. Zhu, S.H. Li, J. He, Mater. Sci. Eng. A **680**, 54-63 (2017).

[31] H.S. Park, J.C. Han, N.S. Lim, J.B. Seol, C.G. Park, Mater. Sci. Eng. A **627**, 262-269 (2015).

[32] I. Timokhina, P. Hodgson, E.V. Pereloma, Metall. Mater. Trans. A **35**, 2331-2341 (2004).

[33] A. Das, M. Ghosh, S. Tarafder, S. Sivaprasad, D. Chakrabarti, Mater. Sci. Eng. A **680**, 249-258 (2017).

[34] A. Grajcar, A. Kozłowska, K. Radwański, A. Skowronek, Metals, **9**, doi:10.3390/met9121304 (2019).

[35] K. Sugimoto, M. Misu, M. Kobayashi, H. Shirasawa, ISIJ Int. **33**, 775-782 (1993).

[36] L. Luo, W. Li, L. Wang, S. Zhou, X. Jin, Mater. Sci. Eng. A **682**, 698-703 (2017).

[37] R. Tian, L. Li, B.C. De Cooman, X.C. Wei, P. Sun, J. Iron Steel Res. Inst. **13**, 51-56 (2006).

[38] A. Kozłowska, A. Janik, K. Radwański, A. Grajcar, Materials, **12**, doi:10.3390/ma12183042 (2019).